Science of the Total Environment 627 (2018) 1–10

Contents lists available at ScienceDirect

Science of the Total Environment

journal homepage: www.elsevier.com/locate/scitotenv

Multistressor effects on river biofilms under global change conditions

Ferran Romero [a,*], Sergi Sabater [a,b], Xisca Timoner [a], Vicenç Acuña [a]

[a] Catalan Institute for Water Research (ICRA), Carrer Emili Grahit 101, 17003 Girona, (Spain)
[b] Institute of Aquatic Ecology, University of Girona, 17071 Girona, (Spain)

HIGHLIGHTS

- River ecosystems are often affected by a combination of chemical and physical stressors.
- A full factorial design revealed the short-term effects of four stressors on river biofilms.
- Responses to stressors combination were 85.5% additive and 14.5% non-additive.
- Non-additive responses were classified as antagonisms (75%) and synergisms (25%).

GRAPHICAL ABSTRACT

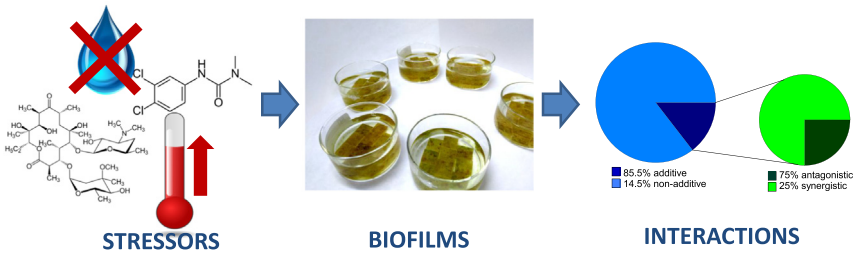

ARTICLE INFO

Article history:
Received 30 November 2017
Received in revised form 16 January 2018
Accepted 16 January 2018
Available online xxxx

Editor: D. Barcelo

Keywords:
Biofilms
Multiple stressors
Microcosms
Water stress
Antagonism

ABSTRACT

Freshwater ecosystems are confronted with multiple chemical, biological and physical stressors. Co-occurring stressors commonly result in additive responses, but non-additive interactions may also occur, hindering our predicting capacity. Despite growing interest in multiple stressor research, the response of freshwater communities to co-occurring chemical and climate change-related physical stressors remains largely unexplored. Here, we used a microcosm approach to evaluate the effect of the combined action of chemical and physical stressors on river biofilms. Results showed that additive responses dominated, whereas 14.5% of all responses were non-additive (75% antagonisms and 25% synergisms). Among these non-additive interactions, physical stressors dominated over chemicals and drove the overall responses. Overall, the occurrence of these non-additive interactions, together with the dominance of the climate-change related physical stressors, might lead to unexpected responses as a result of climate change.

1. Introduction

Unravelling the mechanisms by which aquatic biota respond to global change is still an ongoing major challenge. Current predictions indicate that freshwater communities will face increased physical stress (higher water temperature and desiccation events) (IPCC, 2014), as well as chemical stressors of anthropogenic origin, such as pesticides and pharmaceutical products (Rodriguez-Mozaz et al., 2004; Kuzmanovic et al., 2015). These stressors co-occur in freshwater systems and cause unknown impacts on multiple levels of biological organization, from individual genotypes to communities (Segner and Sabater, 2014). The effects produced by these stressors can be additive, when the effect of the combined action of two or more stressors is equal to the sum of the individual effects, or non-additive (Folt et al., 1999). The latter is further

* Corresponding author at: Catalan Institute for Water Research (ICRA), Carrer Emili Grahit 101, Edifici H2O, Parc Científic i Tecnològic de la Universitat de Girona, E- 17003 Girona, (Spain).
E-mail address: fromero@icra.cat (F. Romero).

https://doi.org/10.1016/j.scitotenv.2018.01.161
0048-9697/

depicted in antagonism or synergism, depending on the negative (antagonism) or positive (synergism) interaction that one stressor has on the other (Crain, 2008; Piggott, Townsend et al., 2015).

Recent analyses have emphasized that interactions in freshwater ecosystems may account for 40% to 69% of all ecological responses (Jackson et al., 2016; Schinegger et al., 2016) and that additive interactions may be as frequent as non-additive interactions (Nõges et al., 2016). A recent literature review suggested that the observed differences may depend on the ecosystem type and the organization level studied, from individual species to populations and whole ecosystems (Côté et al., 2016). Still, uncertainty persists over the combined impacts of multiple stressors from a climate change perspective (Christensen et al., 2006; Ormerod et al., 2010). Field-based approximations often lead to unclear results, due to the confounding effect of natural variability in freshwater ecosystems (Ponsatí et al., 2016). More solid cause-effect relationships can be established using experimental microcosms. These are simplifications of reality that allow for reduced natural variability and increased replication capacity. Although experimental designs using microcosms often use single-species approaches, more reliable results can be obtained if moving towards community-based analysis (Sabater et al., 2007). River biofilms incorporate species with different roles and functions, with autotrophs and heterotrophs co-existing in a highly complex entity. Because of its rapid response to perturbation and major role in nutrient cycling and ecosystem stability, they represent a good candidate to approach the impact of multiple stressors on rivers and streams (Sabater et al., 2007).

Here, we experimentally manipulated two physical stressors (water temperature and desiccation) and two chemical stressors (an herbicide and an antibiotic) in a full factorial model using river biofilms as a model community. Physical stressors were applied following scenarios of future climate change (IPCC, 2014), whereas chemical stressors were applied following realistic worst-case current scenarios (Hirsch et al., 1999; Rabiet et al., 2010). Among chemical stressors, diuron and erythromycin were selected because of their toxicity and occurrence in the environment. Diuron is a phenylurea herbicide widely used to control broadleaf in vineyard areas and flower gardens. Its mode of action is through the blockage of the chloroplast electron transport chain at the photosystem II (*PSII*) level, ultimately leading to the inhibition of photosynthesis (Moreland, 1980). Its concentration in the environment ranges from <1 μg L^{-1} to 10 μg L^{-1} during flood events (Rabiet et al., 2010). Erythromycin is a macrolide considered a wide-spectrum antibiotic against gram-positive and some gram-negative bacteria. The mode of action of erythromycin is through binding to the 23S rRNA molecule in the 50S subunit of the bacterial ribosome, which then blocks the elongation in growing peptide chains, thus inhibiting protein synthesis (Prescott et al., 2000). Erythromycin is commonly found in freshwater ecosystems and, although its concentration is on average low, it may be present at >5 μg L^{-1} at sewage treatment plant effluents (Hirsch et al., 1999).

This study aimed to evaluate the combined impact of 4 stressors on river biofilms. A main question was to determine whether these stressors lead to additive or non-additive responses. We hypothesized that: (i) chemical stressors will have targeted effects on specific biofilm components, consistent with their specific mode of action (ii) physical stressors will mostly have generalized effects, producing non-specific alteration in the selected response variables (iii) desiccation will affect the overall performance of biofilm algae and bacteria, making them sensitive to chemical stress (iv) higher water temperature will oppose the negative effect of chemical stressors by enhancing biofilm metabolism and (v) when occurring, non-additive responses will mostly be antagonistic, given the adaptation of river biofilms to high natural variability (Jackson et al., 2016), therefore showing an inherent capacity to adapt to multiple stressor effects.

2. Material and methods

2.1. Experimental design

We used glass microcosms in an experimental design that followed a full factorial replicated ($n = 4$) design with four factors and two levels per factor (2^4): erythromycin (E), diuron (D), desiccation (W) and water temperature (T) (Fig. 1). Both chemical stressors (E and D) were applied at nominal concentrations of 10 μg L^{-1}. These represent environmentally realistic concentrations though in the higher rank (Hirsch et al., 1999; Rabiet et al., 2010). Temperature was increased by 7 °C according to the predictions of short-term climatic extreme events (IPCC, 2014). Desiccation was applied by letting biofilms air-dry for 4 h. This caused a 70% decrease in photosynthetic efficiency, equivalent to that occurring under field-conditions after 5–6 days of complete desiccation (Acuña et al., 2015; Timoner et al., 2012).

Biofilms were exposed to the stressors over 40 h (impact period), and immediately allowed to recover for 40 h (recovery period) by removing all stressors. Biofilm response to multiple stressors was assessed at the end of the impact and the recovery periods using a variety of structural and functionally-related variables. Basal fluorescence (F_0) and ash-free dry weight (AFDW) were used as a surrogate of algal and total biofilm biomass, respectively (Sabater et al., 2007). Photosynthetic efficiency (Y_{eff}), photosynthetic capacity (Y_{max}) and non-photochemical quenching (NPQ) were used as photosynthetic descriptors of the primary producers in the biofilm. Y_{eff} and Y_{max} respectively indicate the effective and optimal photosynthetic activity, whereas NPQ indicates the algal capacity to dissipate light excess during stress conditions (Ponsatí et al., 2016). Leucine aminopeptidase activity (LAPA) relates to the biofilm capacity to transform dissolved organic nitrogen into inorganic compounds (Ylla et al., 2014). Community respiration (CR) accounts for the capacity of the biofilm community to oxidize organic compounds (Corcoll et al., 2015). Finally, the abundance of three gene transcripts was assessed by quantitative PCR (Smith and Osborn, 2009). The abundance of 16S rRNA and 18S rRNA gene transcripts was used to determine the status of bacterial and eukaryotic communities, respectively. The abundance of *psbA* gene transcript was used as a surrogate of the activity of the autotrophic compartment, as it codes for the D1 protein, which is the main component of the photosystem II (*PSII*) (Kim Tiam et al., 2012).

2.2. Experimental conditions

Each microcosm consisted on an independent glass crystallizer (diameter = 7 cm, height = 4 cm) filled with 100 mL of water and 10 colonized glass slides. Biofilms were grown in artificial channels (see details at Corcoll et al., 2015) for 4 weeks using an inoculum from a non-impacted reference water body, the Llémena river (Sant Esteve

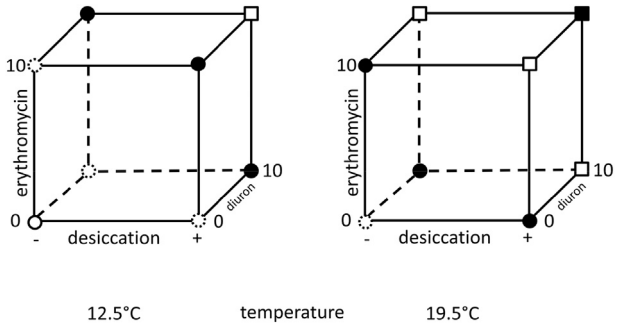

Fig. 1. Experimental design used in this study: full-factorial design with 4 factors and 2 levels per factor. The solid white circle represents the control case. Main effects are represented by dotted circles, 2-way interactions by solid black circles, 3-way interactions by solid squares and the 4-way interaction is represented by a solid black square. Concentrations are indicated in μg L^{-1}.

de Llémena, Girona, EU), which is a permanent Mediterranean river draining a calcareous mountainous range ($d_{50} = 0.74$ mm). After 4 weeks of growth, biofilms were transferred to experimental microcosms. Source water for artificial channels and microcosms was rainwater, filtered through activated carbon filters. During the whole experiment (i.e. 4 weeks of growth, 40 h of exposure and 40 h of recovery), daily cycles of photosynthetic active radiation (PAR) were defined as 12 h daylight and 12 h darkness, and were simulated by LED lights (Lightech, Girona, EU). PAR was held constant at 173.99 ± 33 μE m^{-2} s^{-1} during the daytime, and was recorded every 10 min using quantum sensors (sensor LI-192SA, LiCOR Inc., Lincoln, USA).

We assessed the similarity between the microbial community structure of the microcosms and that of the Llémena River. Thus, biofilm samples were collected after the 4-week growth period in the laboratory to perform DNA extraction (FastDNA® SPIN kit for soils, MP Biomedicals) and 16S rDNA amplicon sequencing, using the Illumina MiSeq platform available at the Research Technology Support Facility of the Michigan State University, USA (Kozich et al., 2013). A presence-absence analysis based on operational taxonomic units (OTUs) revealed that the community used in this study contained 92% of the OTUs present at the Llémena River. Moreover, a parsimony test revealed that the assessed communities were not statistically different (p-value of the maximum parsimony test = 0.306).

2.3. Water chemistry

Water samples were taken before and after the exposure period for chemical analyses of nutrients (phosphate, nitrate and ammonium) and contaminants (diuron and erythromycin).

2.3.1. Nutrients

30 mL of water were filtered through 0.7 μm glass fibre filters (Whatman GF/F, Kent, UK) into pre-washed polyethylene containers. The concentration of phosphate was determined colorimetrically using a fully automated discrete analyzer Alliance Instruments Smartchem 140 (AMS, Frépillon, France). The concentrations of nitrate and ammonium were determined on a Dionex ICS-5000 ion chromatograph (Dionex Corpo- ration, Sunnyvale, U.S.A.).

2.3.2. Erythromycin

Erythromycin (CAS 114-07-8, mol. weight 733.93 g mol^{-1}, Sigma Aldrich) analysis was performed on 10 mL water samples by on-line solid-phase extraction (SPE) ultra-high-performance-liquid chromatography coupled to a triple quadrupole mass spectrometer (UHPLC–MS–MS). Fully automated on-line pre-concentration of erythromycin samples, aqueous standards and operational blanks were analyzed using EQuan MAXTM technology coupled to a TSQ Vantage triple quadrupole mass spectrometer (Thermo Fisher Scientific) (on-line SPE-UHPLC- MS-MS) equipped with an electrospray ionization source (ESI) (Farré et al., 2016).

2.3.3. Diuron

Stock solution of diuron (CAS 330-54-1, mol. weight 233.09 g mol^{-1}, Sigma Aldrich) was prepared on a weight basis, in methanol at 1 mg mL^{-1} and kept frozen at −20 °C. Working standard solution as well as the calibration standard curve was prepared by appropriate dilution in methanol–water (10:90, v/v) of the stock solution of diuron. The samples collected were filtered through 0.45 μm Polyvinylidene fluoride membrane filters (PVDF, Millipore) and analyzed directly by ultraperformance liquid chromatography (UPLC; Waters Corp. Milford, MA, USA) coupled to an hybrid quadrupole-linear ion trap mass spectrometer (5500 QTRAP, Applied Biosystems, Foster City, CA,USA) (LC-MS/MS system) (Ricart et al., 2009).

2.4. Biofilm analyses

2.4.1. Leucine aminopeptidase activity

The degradation capacity of nitrogen compounds was assessed by means of the extracellular enzyme leucine aminopeptidase activity (LAPA). It was measured by means of fluorescent-linked substrata (aminomethyl-coumarin [AMC]). Colonized glass slides were incubated for 1 h in the dark at 12.5 °C immediately after collection. Blanks and standards of AMC (0–100 μmol L^{-1}) were also incubated. At the end of the incubation, glycine buffer (pH 10.4) was added (1/1 vol/vol), and the fluorescence was measured at 364/445 nm excitation/emission for AMC. Values were expressed as nmol of released AMC cm^{-2} h^{-1}.

2.4.2. Community respiration

Community Respiration (CR) was assessed to evaluate bacterial community overall performance by means of the MicroResp™ (Tlili et al., 2011). Briefly, 500 μL of biofilm suspension were obtained by scraping biofilm off glass substrata and resuspending it in 0.2 μm Nuclepore-filtered control water. Biofilm suspension was then used to fill the 96 deep-well microplate coupled to a detection gel. Once assembled, the entire system (biofilm-containing microplate and detection gel) was incubated in the dark (to avoid any photosynthesis interference with CO_2 release) at control temperature (12.5 °C) overnight (15 h).

2.4.3. Ash-free dry weight

A known surface of biofilm (2.25 cm^2) was scrapped from the glass substrata and filtered through a combusted glass fibre filter (Whatman GF/F, Kent, UK). Filters were dried at 70 °C until constant weight and later combusted at 450 °C for 4 h to estimate the ash free dry weight (AFDW).

2.4.4. In vivo Fluorescence measurements

Two glass slides in each replicate were used to evaluate maximum chlorophyll-a fluorescence, photosynthetic efficiency, photosynthetic capacity, and non-photochemical quenching (NPQ). Chlorophyll-a fluorescence, Effective quantum yield (Y_{eff}) and maximum photosynthetic capacity (Y_{max}) were determined in vivo using a Diving PAM (Pulse Amplitude Modulated) underwater fluorometer (Heinz Wlaz, Effeltrich, Germany). Intact glass slides were kept for 30 min in the dark to obtain the maximum chlorophyll-a fluorescence (F_0) and Y_{max}. Y_{eff} and Y_{max} were used as indicators of photosynthetic efficiency and maximal photosynthetic capacity, respectively (Timoner et al., 2012). NPQ was used as an indication of the algal capacity to dissipate the excess light during stress conditions and was calculated following $NPQ = (F_m - F_m')/F_m'$ (Bilger and Bjorkman, 1990), where F_m' represents the maximum chlorophyll fluorescence in steady-state conditions and F_m represents the maximum chlorophyll-a fluorescence under dark-adapted conditions.

2.5. Molecular analyses

2.5.1. RNA extraction

Total RNA was extracted according to the manufacturer's instructions (PowerBiofilm™ RNA isolation kit, MO BIO laboratories). Briefly, 2.25 cm^2 of biofilm were removed from the colonized glass slides using a razor blade and put in 1.5 mL vials. Vials were then centrifuged at 13000*g* during 60 s in order to remove excess water. Biofilms were then added to the PowerBiofilm™ Bead Tube then heated to activate lysis components. Lysis was accomplished through vortex mixing using a Vortex Adapter for Vortex-Genie® 2 (MO BIO laboratories), followed by protein and inhibitor removal. Total RNA was then captured on a flat bottom silica spin column and eluted on 50 μL of sterile ultrapure water.

2.5.2. RNA purification (DNAse treatment)

Total RNA (50 μL) was purified using a commercial kit according to the manufacturer's instructions (TURBO DNA-*free*™, Ambion®). Briefly,

5 μL of TURBO DNAse buffer and 1 μL of TURBO DNAse were added to 50 μL of RNA. DNAse activity was performed at 37 °C during 30 min. Purified RNA was kept at −80 °C until further proceeding.

2.5.3. Reverse transcription of RNA

The first strand of complementary DNA (cDNA) was synthesized from 1 μL of total purified RNA using the SuperScript® III First-Strand Synthesis System. The RNA-primer mixture contained 1 μL of total RNA, 1 μL of random hexamers (50 ng μL^{-1}), 1 μL of 10 mM dNTP mix and 7 μL of DEPC-treated water. The RNA-primer mixture was incubated at 65 °C for 5 min. The synthesis mix contained (per sample): 2 μL of 10× RT buffer, 4 μL of 25 mL $MgCl_2$, 2 μL of 0.1 M DTT, 1 μL of RNAseOUT® (40 U/μL) and 1 μL of SuperScript® III RT (200 U/μL). The synthesis mix was added to the RNA-primer mixture and incubated at 25 °C for 10 min, followed by 50 min at 50 °C. The cDNA mixture was conserved at −20 °C until it was used in quantitative real-time PCR.

2.5.4. Quantitative PCR

Quantitative real-time PCR (qPCR) was performed on an Mx3005P system (Agilent Technologies, Santa Clara, CA, USA) following the manufacturer's instructions by means of SYBR Green detection chemistry. Accordingly, 1 activation cycle was performed during 3 min at 95 °C, followed by 50 amplification cycles at 95 °C for 15 s and 60 °C for 60 s. Each 30.4 μL reaction contained 15 μL of SYBR-green mix, 12 μL of DEPC-treated water, 1.2 of forward primer (10 mM), 1.2 of reverse primer (10 mM) and 1 μL of template cDNA. For negative controls, cDNA was replaced by DEPC-treated water. Three genes were quantified from cDNA; (i) 16S rRNA gene, coding for the main component of the small subunit of prokaryotic ribosomes, was here used as a surrogate of bacterial overall performance; (ii) 18S rRNA gene, coding for the main component of the small subunit of eukaryotic ribosomes, was used as a surrogate of eukaryotic (mainly algal) performance; (iii) *psbA* gene, coding for the D1 protein, which is a central component of the photosystem II, was used as a surrogate of overall photosynthetic activity. Specificity was determined for each reaction from the dissociation curve of the PCR product. This dissociation curve was obtained by following the SYBR Green fluorescence level during a gradual heating of the PCR products from 60 to 95 °C. More details about qPCR are described on Table S1 and Table S2. Absolute quantification of each gene expression level was performed using a standard curve.

2.5.5. Standard curve set-up for qPCR absolute quantification

16S rDNA, 18S rDNA and *psbA* genes were amplified from biofilm-extracted DNA (PowerSoil™ DNA isolation kit, MO BIO laboratories) by conventional PCR. PCR products were immediately cloned into *Escherichia coli* competent cells using the StrataClone PCR cloning kit (Agilent Technologies). Basically, fresh PCR products were incubated with Topoisomerase I-charged vector arms for 5 min and then heat-shock transformed for 60 s into competent cells expressing Cre recombinase. Screening of transformants was realized on ampicilline-containing LB medium agar plates. Selected colonies were used for plasmid extraction using a regular commercial kit (PureLink® Quick Plasmid Miniprep Kit, Invitrogen). The presence of the plasmid on the final product was verified by PCR. The presence of the genes on the final product was verified by Illumina sequencing (MacroGen Inc.) of PCR products. Standard curves for qPCR were obtained by simple dilution of the plasmid-containing final extract.

2.6. Statistical analyses

Generalized linear model (GLM) analyses were conducted in R software version 3.3.0 (R Core Team, 2017) using the *glm* default function. Erythromycin (E), diuron (D), desiccation (W) and water temperature (T) were fixed as categorical factors with 2 levels per factor (i.e. presence vs. absence of the stressor). Response parameters Y_{eff}, Y_{max}, NPQ, F_0, LAPA, CR, AFDW, 16S, 18S and psbA were fixed as response variables. The model included all interaction terms (up to 4th order). We selected type III sum of squares, as recommended for this type of studies (Garson, 2015) and significance level for all tests was set at $p < 0.05$.

Two types of effects were calculated from the GLM: *Main effects* compared the mean performance in the treatments where a given stressor is present versus the treatments where the stressor is absent. Main effects were classified as positive (+) if the presence of the stressor significantly increased the overall response of the corresponding variable or negative (−) if the stressor significantly decreased the overall response of the corresponding variable. *Interactive effects* were calculated following Crain, 2008 and indicated when an interaction between two or more stressors occurred. Interactive effects were classified depending on the combined effect of the interacting stressors: antagonism (A) was assumed when the combined effect was less than predicted additively, whereas synergism (S) was assumed when the combined effect was more pronounced than predicted additively. To evaluate the recovery of the biofilm responses, a classic one-way ANOVA was used to compare the response after the impact and recovery phases.

As GLM is a null hypothesis significance testing approach, it only provides us with evidence against the null hypothesis (i.e. the *p-value*). Null hypothesis significance testing does not provide us with an estimate of the magnitude of the effect of interest. Consequently, we used the *etaSquared* default function in R Software to calculate the effect size (ES), a correlation statistic which estimates the magnitude of an effect as the percentage of variance accounted for by a given treatment (Nakagawa and Cuthill, 2007). Effect size was calculated as the ratio between the type III sum of squares (SS) of a given factor and the type III SS of this factor + the type III SS of the error. Accordingly, an ES of 0 means no relationship whatsoever between a treatment and a response parameter, whereas an ES of 1 means a perfect relationship.

3. Results

3.1. Water chemistry

Diuron and erythromycin were both detected in microcosm water samples at levels near the nominal concentration (Table 1). After the exposure period (40 h), the concentration of diuron was significantly lower (4.9 μg L^{-1}) than before the beginning of the experiment. Nitrate and phosphate were detected at lower concentrations after the exposure period, whereas the concentration of ammonium increased (Table 1).

3.2. Single stressor effects

Physical stressors desiccation (W) and temperature (T) had the most pervasive effects: the two affected ca. 50% of variables (significant main effects). Desiccation had the strongest effect, with an effect size (ES) between 0.03 and 0.54. The chemical stressors erythromycin (E) and diuron (D) significantly affected 20% and 10% of the variables, respectively. Diuron had the highest effect size of the two (ES = 0.30).

Erythromycin produced a significant positive main effect on community respiration (CR) (Table 2), which increased by 64.65% (relative to the control), and negatively affected the abundance of 16S rRNA, which decreased by 67.4% (Fig. 2). CR recovered significantly and was only 1.6% less than the control after the recovery period (Fig. 3). The 16S rRNA gene expression also recovered, but remained 29.3% less than the control (Fig. 3). Diuron had a main negative impact on photosynthetic efficiency (Y_{eff}) (Table 2). Exposure to diuron reduced Y_{eff} by 32.9% (Fig. 2), but it significantly recovered ($p < 0.05$ in one-way ANOVA) after the recovery period (Fig. 3).

Desiccation had a main negative effect on all photosynthetic parameters, as well as leucine aminopeptidase activity (LAPA) (Table 2). Photosynthetic efficiency and photosynthetic capacity (Y_{eff} and Y_{max}) significantly recovered, being 29.3% and 11% higher than the control

Table 1
Water chemistry information at the beginning (t_{0h}) and the end (t_{40h}) of the exposure period. For water toxicants (i.e. diuron and erythromycin), concentrations are given in μg L^{-1}, for nutrients (i.e. NO_3^-, PO_4^- and NH_4^+) concentrations are given in mg L^{-1}. The asterisk indicates a significant difference (Tukey's test p-value < 0.05 in a one-way ANOVA) in the toxicant or nutrient concentration detected in microcosm water before and after 40 h of exposure.

Experimental phase	Diuron (μg L^{-1})	Erythromycin (μg L^{-1})	Nitrate (NO_3^-) (mg L^{-1})	Phosphate (PO_4^-) (mg L^{-1})	Ammonium (NH_4^+) (mg L^{-1})
t_{0h}	11.7 ± 1.5	9.2 ± 2.9	1.97 ± 0.48	0.01 ± <0.01	<0.01
t_{40h}	4.9* ± 0.8	10.8 ± 3.7	0.37* ± 0.02	<0.01	0.34* ± 0.02

after the recovery period (Fig. 3). Temperature had a main negative effect on Y_{max}, non-photochemical quenching (NPQ) and the expression of *psbA*, but it increased the basal fluorescence (F_0) and the LAPA (Table 2). Temperature acting individually decreased Y_{max} by 22.7% and NPQ by 68.1%, whereas it increased F_0 by 22.6% and LAPA by 33.4% (Fig. 2). Y_{max} and NPQ showed significant recovery (10.2% and 39.4% lower than the control after the recovery period, Fig. 3).

3.3. Multiple stressor effects

The interaction between stressors ranged from additive to significant 2-way and higher-order interactions. Among all combinations, 85.5% produced additive responses, whereas 14.5% resulted in non-additive interactions. Of these, 75% were classified as antagonisms and 25% as synergisms. The most pervasive interactions involved physical stressors. Desiccation and increased temperature (WT) resulted in significant interactions for 50% of the studied variables. This combination also resulted in significant interactions when chemical stressors were considered, both in 3-way (DTW and ETW) and 4-way (DEWT) combinations.

Diuron and desiccation acting jointly synergistically reduced photosynthetic capacity (Y_{max}), which was 67.8% lower than the control after the impact period, and recovered up to 8.8% after the recovery period; Figs. 2 and 3. The interaction between diuron and temperature caused the antagonistic reduction of photosynthetic efficiency, Y_{eff} (19.9% of the control; much less than the predicted additive decrease of 40.4%). Y_{eff} recovered up to 0.6% lower than the control. Erythromycin and temperature antagonistically decreased F_0 by 12.5% (Table 2), also diverging from the additive prediction of a 30.7% increase. F_0 increased by 47.9% after recovery. The triple combination of diuron, erythromycin and temperature increased 16S rRNA and *psbA* expression, the interaction being antagonistic in both cases.

Desiccation and temperature resulted in significant interactions for photosynthetic parameters and LAPA. The additive prediction was that Y_{eff} and Y_{max} should decrease by 40.4% and 46.4% in this, but both increased by 89.4% and 37.0% compared to the control, respectively. The combination between desiccation and increased temperature also caused a 76.1% increase in community respiration. The three variables remained higher than the control (54.1%, 26.2% and 18.3%, respectively) after the recovery period. NPQ and F_0 were also reduced by 76.0% and 65.4% compared to the control, respectively, and the LAPA by 27.1% (Fig. 2). NPQ, F_0 and LAPA remained 71.7%, 59.9% and 21.1% lower than control values after recovery.

Diuron, temperature and desiccation altogether had significant effects on Y_{eff} and NPQ. The additive outcome predicted a decrease in Y_{eff} and NPQ while they increased by 9.3% and 33.2%, respectively. The NPQ approached control values after the recovery period, but Y_{eff} remained 82.2% higher.

Erythromycin, temperature and desiccation resulted in a synergistic decrease of basal fluorescence (F_0), whereas the interaction was antagonistic for AFDW and 16S rRNA gene expression. In all cases, the deviation was maintained after recovery. Last, the 4-way interaction between diuron, erythromycin, desiccation and temperature synergistically increased the expression of *psbA* by 65.3% and shifted to 54.5% lower than control after recovery.

Table 2
Summary of GLMs (p-values) comparing response variables across experimental treatments. Effect sizes are shown in parentheses for cases where p-value < 0.05. Significant main effects (+, positive, −, negative) and interactions (A, antagonism, S, synergism) are indicated.

	E	D	W	T	DE	DW	DT	EW	WT	ET	DTW	ETW	DEW	DET	DEWT
Y_{eff}	0.17	**<0.001 (0.30) −**	**<0.001 (0.30) −**	0.28	0.16	0.58	**0.05 (0.08) A**	0.22	**<0.001 (0.76) A**	0.46	**<0.001 (0.34) A**	0.41	0.58	0.26	0.49
Y_{max}	0.14	0.64	**0.001 (0.20) −**	**0.002 (0.18) −**	0.43	**<0.001 (0.27) S**	0.20	0.53	**<0.001 (0.60) A**	0.21	0.76	0.77	0.13	0.55	0.32
NPQ	0.87	0.86	**0.001 (0.20) −**	**<0.001 (0.23) −**	0.36	0.73	0.17	0.38	**0.04 (0.089) A**	0.98	**0.04 (0.087) A**	0.61	0.55	0.80	0.19
F_0	0.33	0.14	**<0.001 (0.54) −**	**0.008 (0.14) +**	0.58	0.17	0.10	0.26	**0.02 (0.10) S**	**<0.001 (0.23) A**	0.25	**0.01 (0.12) S**	0.47	0.11	0.29
LAPA	0.54	0.65	**0.008 (0.14) −**	**0.002 (0.18) +**	0.88	0.63	0.33	0.06	**0.04 (0.09) S**	0.38	0.76	0.13	0.29	0.25	0.94
AFDW	0.29	0.88	0.91	0.66	0.34	0.38	0.52	0.17	0.17	0.12	0.63	**0.02 (0.10) A**	0.45	0.08	0.12
CR	**0.03 (0.09) +**	0.07	0.19	0.70	0.35	0.16	0.13	0.14	0.24	0.17	0.40	0.29	0.95	0.22	0.20
16S rRNA	**0.04 (0.10) −**	0.15	0.37	0.88	0.20	0.71	0.98	0.42	0.86	0.78	0.66	**0.02 (0.11) A**	0.58	**0.05 (0.09) A**	0.07
18S rRNA	0.82	0.84	0.55	0.97	0.91	0.71	0.79	0.55	0.91	0.67	0.42	0.33	0.80	0.23	0.21
psbA	0.10	0.39	**0.04 (0.03) −**	**0.04 (0.03) −**	0.57	0.80	0.25	0.26	0.16	0.09	0.38	0.25	0.38	**<0.001 (0.14) A**	**<0.001 (0.11) A**

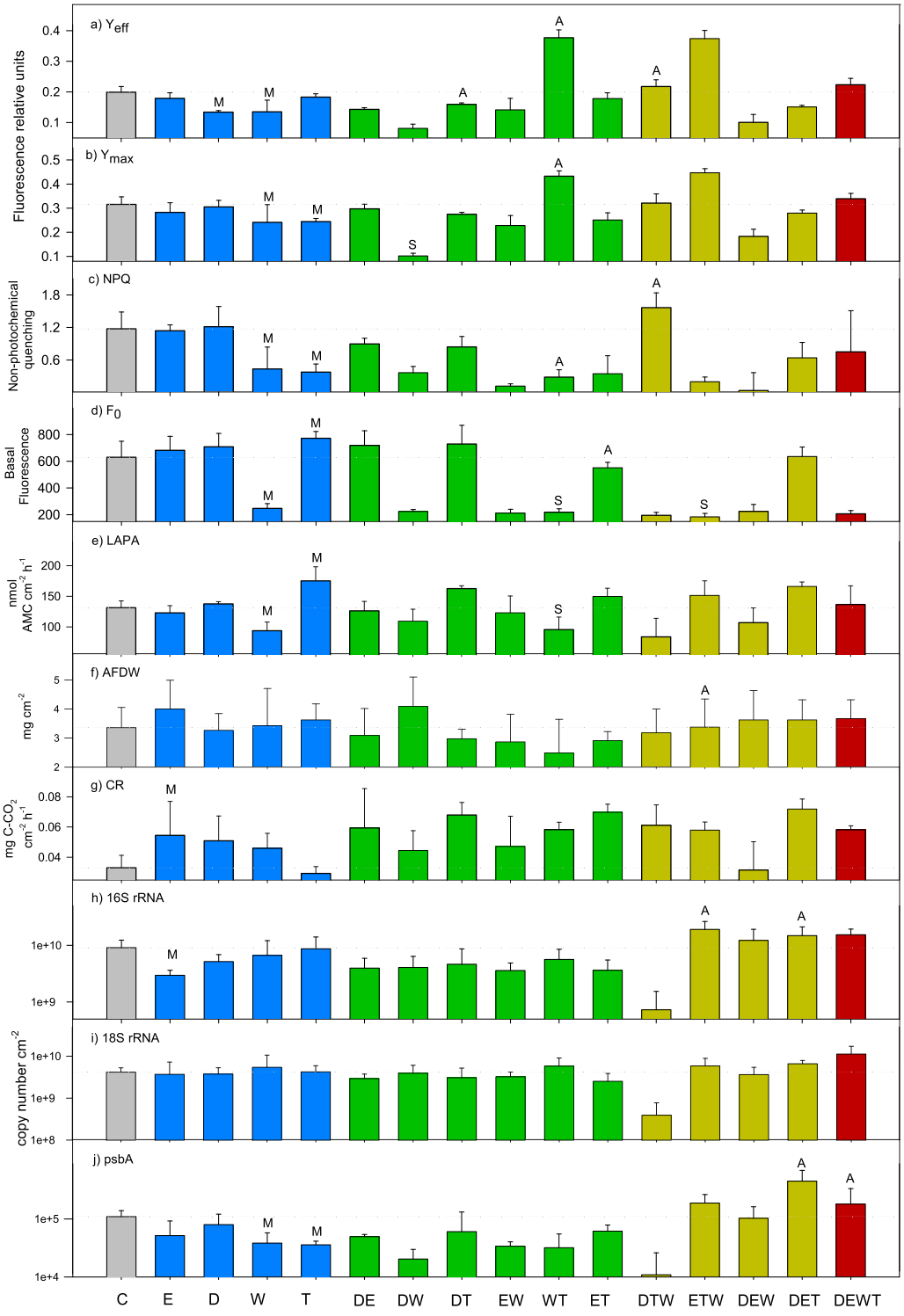

Fig. 2. Average of Photosynthetic Efficiency (a), Maximum Photosynthetic Capacity (b), Non-Photochemical Quenching (c), Basal Fluorescence (d), Leucine Amino-Peptidase Activity (e), Ash Free Dry Weight (f), Community Respiration (g), 16S rRNA copy number (h), 18S rRNA copy number (i), and *psbA* copy number (j). Error bars (SEs) show variation between replicates ($n = 4$). Grey bar (C) shows control treatment (no stress). Significant main effects (M) are indicated for single stressors (E, erythromycin; D, diuron; W, desiccation and T, temperature). Significant interactions are indicated as A (antagonism) or S (synergism). Dotted dash line allows rapid comparison with control value.

4. Discussion

4.1. Considerations on the followed approach

Our microcosms approach has the advantage of combining rigorous control over ecological stressors and sufficient power to detect both main effects and interactions. We were sufficiently able to reproduce the biofilm community growing on the reference site in terms of bacterial diversity (as demonstrated by OTUs analyses, see Section 2.2 Experimental conditions). However, the biofilm community used in this study did not contain any consumers (e.g. grazers), so we could not predict any effects across the food web. Importantly, the exposure to selected stressors was short and acute. While chronic stress exposure usually leads to adaptation of the community, as sensitive species are replaced

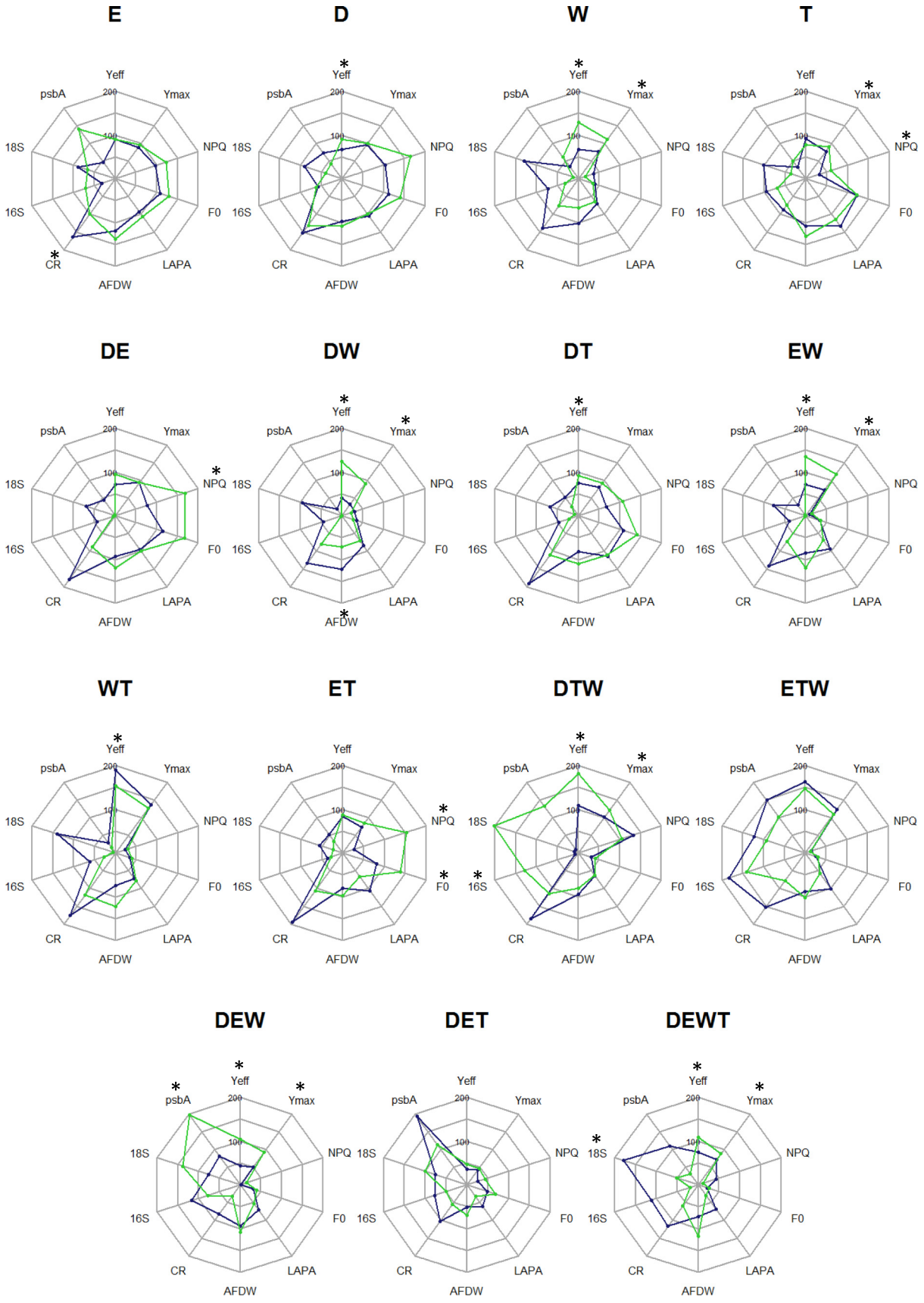

Fig. 3. Response variables across treatments. The results are indicated as percentage of the control. Dark blue line indicates percentages obtained after exposure to stressors. Light green line indicates percentages obtained after recovery period under stress-free conditions. Asterisks show significant (p-value < 0.05) difference between exposure and recovery periods. (For interpretation of the references to colour in this figure legend, the reader is referred to the web version of this article.)

by tolerant species, our approach consisted of an acute exposure to the stressors, likely making adaptation of the community through species succession impossible. This limitation associated with exposure conditions in short-term experiments is in line with the rise of synergisms (Vinebrooke et al., 2004). Also, our experimental design did not allow us to assess multiple stressor effects across different levels of stressors. Changing levels of stressors (e.g. applying chemical stressors at other concentrations) could possibly lead to other main effects and interactions. However, the levels of stressors used in this study represented realistic scenarios.

4.2. Single stressor effects

4.2.1. Chemical stressors

Chemical stressors diuron and erythromycin altered biofilm structure and functioning. Here we have shown how a short-term (40 h) exposure to 10 μg L^{-1} of the herbicide diuron significantly reduced the photosynthetic efficiency of a river biofilm. On the other hand, exposure to 10 μg L^{-1} of the antibiotic erythromycin decreased 16S rRNA gene expression and increased community respiration. These results confirm the hypothesis that chemical stressors would have effects according to their mode of action. The herbicide had a short-term effect on photosynthetic performance but did not compromise the integrity of the photosynthetic apparatus. This was evidenced by the significant alteration of photosynthetic efficiency (Y_{eff}) but not the photosynthetic capacity (Y_{max}). Similar results have been observed for the photosynthetic capacity of multispecies biofilms (Larras et al., 2013). The antibiotic showed general toxicity to bacteria whereas it likely promoted respiration activity due to the selection pressure affecting sensitive species and favouring tolerant non-nutrient limited bacteria (Tello et al., 2012).

4.2.2. Physical stressors

Physical stressors desiccation and increased temperature (7 °C above control) had larger effects than chemical stressors, altering 60% and 50% of the variables, respectively. The altered variables mostly included photosynthesis-related parameters and enzymatic activity (Table 2). These results partially confirm the hypothesis that physical stressors have general effects for algal and bacterial compartments. The prediction was largely supported for desiccation which decreased all photosynthetic parameters (i.e., Y_{eff}, Y_{max}, NPQ, F_0 and the expression of *psbA*), as well as enzymatic activity. Desiccation caused the largest effect size (ES = 0.54). Similar effects were observed in biofilms in field and laboratory experiments (Ylla et al., 2010; Timoner et al., 2012; Proia et al., 2013). The photosynthetic parameters Y_{eff} and Y_{max} were the ones to recover fastest after desiccation, in line with previous studies (Barthès et al., 2014). The prediction that physical stressors will have general effects was only partially fulfilled in the case of temperature stress. Temperature acted as a subsidy for basal fluorescence and enzymatic activity. However, it likely produced a negative effect in the structure of *PSII*, as shown by a decrease in Y_{max}, NPQ and *psbA* expression.

4.3. Multiple stressor effects

Interactive effects were especially pervasive for physical stressors. Desiccation applied as a 4-h drought made biofilms significantly more sensitive to the herbicide diuron, as shown by a synergistic interaction between these stressors. This result is in line with our third hypothesis, which stated that desiccation would make biofilms sensitive to chemical stress. Desiccation produces direct effects on biofilm cells, which could suffer from stress caused by the lack of water and/or osmotic shock, in many cases leading to cell lysis (Schimel et al., 2007). The biofilm was thin and therefore poorly resistant to desiccation. Certainly, thinner biofilms are known to be more sensitive to chemical stress (Cochran et al., 2000; Ivorra et al., 2000). Beyond these structural causes, physiological mechanisms could also be at play. The allocation of resources on a previously disturbed community would shift towards the maintenance of the cellular machinery, e.g. by producing protective molecules such as heat-shock proteins (Maleki, 2016). Under this situation, less energy is available for detoxifying pathways, ultimately making the community more sensitive to chemical stressors (Schimel et al., 2007). These mechanisms together predict that chemical stressors such as herbicides and antibiotics would be more harmful to river biofilms subjected to desiccation. The poor recovery of structural variables confirms that the biofilm structure was heavily affected by desiccation.

Our fourth hypothesis stated that increased temperature would favour functional variables, counteracting the negative effects of chemical stressors. This indeed was the case for the combination between diuron and increased temperature: the negative effects of diuron on photosynthetic efficiency were compensated by temperature. The detrimental effects of diuron were less pronounced when the biofilm was maintained at higher temperature (Fig. 2), possibly as a result of the increase in the turnover rate of the *psbA*-encoding protein D1, which could desensitize *PSII* to the toxic effect of herbicides (Larras et al., 2013). Temperature preferentially affected functional (av. ES = 0.11 ± 0.09) rather than structural variables (av. ES = 0.04 ± 0.07), in line with the effect that temperature has on metabolic processes (Marcus et al., 2014). Chemical stressors showed a similar effect size on autotrophic and heterotrophic variables, but the effect of physical stressors (especially desiccation) was more pronounced on autotrophic (av. ES = 0.12 ± 0.06) rather than heterotrophic variables (av. ES = 0.06 ± 0.02).

The strongest interaction occurred between physical stressors. The combination of desiccation and temperature resulted in a sharp increase in photosynthetic performance that mitigated the individual effects. This unpredicted nonlinear interaction was among the strongest and more statistically robust, resulting in an ecological surprise (Ormerod et al., 2010). This interaction suggests that the co-occurrence of desiccation and increased temperature mitigated individual effects. A recent meta-analysis of multiple stressor effects in freshwater ecosystems shows that temperature is the stressor most commonly associated with mitigating interactions (Jackson et al., 2016). We argue that increased temperature could activate the metabolism of cells that remain once the negative effect of desiccation has decimated the most sensitive organisms. This activation could favour the per capita use of resources. Increased temperature can rapidly stimulate metabolic activity as long as resources are not limiting, and this might be the case during the re-established early stages of succession after the disturbance (Marcus et al., 2014).

We observed that 50% of non-additive interactions involved at least three stressors. Photosynthetic efficiency (Y_{eff}) was the most affected by diuron, temperature and desiccation, and the resultant Y_{eff} value was higher than its additive prediction. Y_{eff} is reduced by ca. 50% when diuron is added to the interaction between desiccation and temperature. This suggests that while the combination between desiccation and temperature could lead the community back to an early successional stage, the fast-growing communities were more sensitive to herbicides such as diuron. The results, taken together, could be interpreted as an indication that biofilm communities exposed to increased temperature and desiccation due to climate change could be more sensitive to herbicide toxicity.

Our fifth hypothesis stated that antagonism would be the most prevalent response among the non-additive interactions. This hypothesis was confirmed but merits further discussion according to the obtained results. Antagonism represented 75% of all non-additive interactions, whereas synergism represented the 25%. However, non-additive interactions represented only 14.5% of all combinations in the full-factorial model, being additive for 85.5% of all combinations. Manipulative studies using higher-order interactions have found results comparable to the ones we observed (Piggott et al., 2012, Piggott, Niyogi et al., 2015 and Piggott, Townsend et al., 2015). Synergism represented a non-negligible 25% of non-additive interactions, suggesting a role of synergism in a climate change context.

5. Conclusions

Our study reveals that a complex freshwater community may show non-additive responses to multiple stressors when faced with future global change conditions. These responses, driven primarily by physical stressors, may display unexpected outcomes when increased temperature and water stress occur with chemical stressors such as pharmaceutical products or agricultural pesticides. We exposed river biofilms to acute worst-case conditions, and therefore the effect and direction of these interactions may vary in the long term. However, our results show the path to further studies, assessing the effect of these interactions at a chronic scale or across different levels of stress.

Acknowledgements

This study was funded by the Spanish Ministry of Economy and Competitiveness through the project "Temporary fluvial ecosystems and global change: effects on ecosystem structure and functioning" (FUNSTREAM)-CGL2014-58760-C3-3-R. Authors acknowledge insightful comments by the Springer Editing Service, as well as the support from the Economy and Knowledge Department of the Catalan Government through Consolidated Research Group (2014 SGR 291) - Catalan Institute for Water Research. The scientific facilities of ICRA have been cofinanced by the Spanish Ministry of Economy and Competitiveness (MINECO) and by the European Regional Development Fund (ERDF) in the frame of the Catalonia ERDF Operative program 2007–2013.

Competing financial interests

The authors declare no competing financial interests.

Appendix A. Supplementary data

Supplementary data to this article can be found online at https://doi.org/10.1016/j.scitotenv.2018.01.161.

References

Acuña, V., Casellas, M., Corcoll, N., Timoner, X., Sabater, S., 2015. Increasing extent of periods of no flow in intermittent waterways promotes heterotrophy. Freshw. Biol. 60:1810–1823. https://doi.org/10.1111/fwb.12612.

Barthès, A., Ten-Hage, L., Lamy, A., Rols, J.L., Leflaive, J., 2014. Resilience of aggregated microbial communities subjected to drought-small-scale studies. Microb. Ecol. 70:9–20. https://doi.org/10.1007/s00248-014-0532-0.

Bilger, W., Bjorkman, O., 1990. Role of the xanthophyll cycle in photoprotection elucidated by measurements of light-induced absorbance changes, fluorescence and photosynthesis in leaves of *Hedera canariensis*. Photosynth. Res. 25:173–185. https://doi.org/10.1007/BF00033159.

Christensen, M.R., Graham, M.D., Vinebrooke, R.D., Findlay, D.L., Paterson, M.J., Turner, M. A., 2006. Multiple anthropogenic stressors cause ecological surprises in boreal lakes. Glob. Chang. Biol. 12:2316–2322. https://doi.org/10.1111/j.1365-2486.2006.01257.x.

Cochran, W.L., McFeters, G.A., Stewart, P.S., 2000. Reduced susceptibility of thin *Pseudomonas aeruginosa* biofilms to hydrogen peroxide and monochloramine. J. Appl. Microbiol. 88:22–30. https://doi.org/10.1046/j.1365-2672.2000.00825.x.

Corcoll, N., Casellas, M., Huerta, B., Guasch, H., Acuña, V., Rodríguez-Mozaz, S., Serra-Compte, A., Barceló, D., Sabater, S., 2015. Effects of flow intermittency and pharmaceutical exposure on the structure and metabolism of stream biofilms. Sci. Total Environ. 503–504:159–170. https://doi.org/10.1016/j.scitotenv.2014.06.093.

Côté, I.M., Darling, E.S., Brown, C.J., 2016. Interactions among ecosystem stressors and their importance in conservation. Proc. R. Soc. B Biol. Sci. 283, 20152592. https://doi.org/10.1098/rspb.2015.2592.

Crain, C., 2008. Interactions and cumulative impacts of multiple stressors in marine ecosystems. Ecol. Lett. 11:1304–1315. https://doi.org/10.1111/j.1461-0248.2008.01253.x.

Farré, M.J., Insa, S., Mamo, J., Barceló, D., 2016. Determination of 15 N-nitrosodimethylamine precursors in different water matrices by automated on-line solid-phase extraction ultra-high-performance-liquid chromatography tandem mass spectrometry. J. Chromatogr. A https://doi.org/10.1016/j.chroma.2016.06.064.

Folt, C.L., Chen, Y.C., Moore, M.V., Burnaford, J., 1999. Synergism and antagonism amond multiple stressors. Limnol. Oceanogr. 44:864–877. https://doi.org/10.4319/lo.1999.44.3_part_2.0864.

Garson, D., 2015. GLM Multivariate, MANOVA, and Canonical Correlation. Statistical Associates Publishers, Asheboro, North Carolina, USA.

Hirsch, R., Ternes, T., Haberer, K., Kratz, K.L., 1999. Occurrence of antibiotics in the aquatic environment. Sci. Total Environ. 225:109–118. https://doi.org/10.1016/S0048-9697(98)00337-4.

IPCC, 2014. Climate change 2014: impacts, adaptation, and vulnerability. Part A: global and sectoral aspects. In: Field, C.B., Barros, V.R., Dok, D.J. (Eds.), Contribution of Working Group II to the Fifth Assessment Report of the Intergovernmental Panel on Climate Change.

Ivorra, N., Bremer, S., Guasch, H., Kraak, M.H.S., Admiraal, W., 2000. Differences in the sensitivity of benthic microalgae to Zn and Cd regarding biofilm development and exposure history. Environ. Toxicol. Chem. 19, 1332–1339.

Jackson, M.C., Loewen, C.J.G., Vinebrooke, R.D., Chimimba, C.T., 2016. Net effects of multiple stressors in freshwater ecosystems: a meta-analysis. Glob. Chang. Biol. 22:180–189. https://doi.org/10.1111/gcb.13028.

Kim Tiam, S., Feurtet-Mazel, A., Delmas, F., Mazzella, N., Morin, S., Daffe, G., Gonzalez, P., 2012. Development of q-PCR approaches to assess water quality: effects of cadmium on gene expression of the diatom *Eolimna minima*. Water Res. 46:934–942. https://doi.org/10.1016/j.watres.2011.11.005.

Kozich, J.J., Westcott, S.L., Baxter, N.T., Highlander, S.K., Schloss, P.D., 2013. Development of a dual-index sequencing strategy and curation pipeline for analyzing amplicon sequence data on the MiSeq Illumina sequencing platform. Appl. Environ. Microbiol. 79:5112–5120. https://doi.org/10.1128/AEM.01043-13.

Kuzmanovic, M., Ginebreda, A., Petrovic, M., Barceló, D., 2015. Risk assessment based prioritization of 200 organic micropollutants in 4 Iberian rivers. Sci. Total Environ. 503-504:289–299. https://doi.org/10.1016/j.scitotenv.2014.06.056.

Larras, F., Lambert, A.S., Pesce, S., Rimet, F., Bouchez, A., Montuelle, B., 2013. The effect of temperature and a herbicide mixture on freshwater periphytic algae. Ecotoxicol. Environ. Saf. 98:162–170. https://doi.org/10.1016/j.ecoenv.2013.09.007.

Maleki, F., 2016. Bacterial heat shock protein activity. J. Clin. Diagn. Res.:10–12 https://doi.org/10.7860/JCDR/2016/14568.7444.

Marcus, H., Wey, J.K., Norf, H., Weitere, M., 2014. Disturbance alters the response of consumer communities towards warming: a mesocosm study with biofilm-dwelling ciliates. Ecosphere 5, 1–15.

Moreland, D.E., 1980. Mechanisms of action of herbicides. Annu. Rev. Plant Physiol. 31, 597–638.

Nakagawa, S., Cuthill, I.C., 2007. Effect size, confidence interval and statistical significance: a practical guide for biologists. Biol. Rev. 82:591–605. https://doi.org/10.1111/j.1469-185X.2007.00027.x.

Nõges, P., Argillier, C., Borja, Á., Garmendia, J.M., Hanganu, J., Kodeš, V., Pletterbauer, F., Sagouis, A., Birk, S., 2016. Quantified biotic and abiotic responses to multiple stress in freshwater, marine and ground waters. Sci. Total Environ. 540:43–52. https://doi.org/10.1016/j.scitotenv.2015.06.045.

Ormerod, S.J., Dobson, M., Hildrew, A.G., Townsend, C.R., 2010. Multiple stressors in freshwater ecosystems. Freshw. Biol. 55:1–4. https://doi.org/10.1111/j.1365-2427.2009.02395.x.

Piggott, J.J., Lange, K., Townsend, C.R., Matthaei, C.D., 2012. Multiple stressors in agricultural streams: a Mesocosm study of interactions among raised water temperature, sediment addition and nutrient enrichment. PLoS One 7, e49873. https://doi.org/10.1371/journal.pone.0049873.

Piggott, J.J., Niyogi, D.K., Townsend, C.R., Matthaei, C.D., 2015a. Multiple stressors and stream ecosystem functioning: climate warming and agricultural stressors interact to affect processing of organic matter. J. Appl. Ecol. 52:1126–1134. https://doi.org/10.1111/1365-2664.12480.

Piggott, J.J., Townsend, C.R., Matthaei, C.D., 2015b. Reconceptualizing synergism and antagonism among multiple stressors. Ecol. Evol. 5:1538–1547. https://doi.org/10.1002/ece3.1465.

Ponsatí, L., Corcoll, N., Petrovic, M., Picó, Y., Ginebreda, A., Tornés, E., Guasch, H., Barceló, D., Sabater, S., 2016. Multiple-stressor effects on river biofilms under different hydrological conditions. Freshw. Biol. 61:2102–2115. https://doi.org/10.1111/fwb.12764.

Prescott, J.F., Baggott, J., Walker, R., 2000. Antimicrobial Therapy in Veterinary Medicine. Iowa State Univ. Press, Ames, IA, pp. 229–262.

Proia, L., Vilches, C., Boninneau, C., Kantiani, L., Farré, M., Romaní, A.M., Sabater, S., Guasch, H., 2013. Drought episode modulates the response of river biofilms to triclosan. Aquat. Toxicol. 127:36–45. https://doi.org/10.1016/j.aquatox.2012.01.006.

R Core Team, 2017. R: A language and environment for statistical computing. R Foundation for Statistical Computing, Vienna, Austria http://www.R-project.org/.

Rabiet, M., Margoum, C., Carluer, N., 2010. Assessing pesticide concentrations and fluxes in the stream of a small vineyard catchment – effect of sampling frequency. Environ. Pollut. 158:737–748. https://doi.org/10.1016/j.envpol.2009.10.014.

Ricart, M., Barceló, D., Geiszinger, A., Guasch, H., López, M., Alda, D., Romaní, A.M., Vidal, G., Villagrasa, M., Sabater, S., 2009. Effects of low concentrations of the phenylurea herbicide diuron on biofilm algae and bacteria. Chemosphere 76:1392–1401. https://doi.org/10.1016/j.chemosphere.2009.06.017.

Rodriguez-Mozaz, S., López De Alda, M.J., Barceló, D., 2004. Monitoring of estrogens, pesticides and bisphenol a in natural waters and drinking water treatment plants by solid-phase extraction-liquid chromatography-mass spectrometry. J. Chromatogr. A 1045:85–92. https://doi.org/10.1016/j.chroma.2004.06.040.

Sabater, S., Guasch, H., Ricart, M., Romaní, A., Vidal, G., Klünder, C., Schmitt-Jansen, M., 2007. Monitoring the effect of chemicals on biological communities. The biofilm as an interface. Anal. Bioanal. Chem. 387:1425–1434. https://doi.org/10.1007/s00216-006-1051-8.

Schimel, J., Balser, T.C., Wallenstein, M., 2007. Microbial stress-response physiology and its implications for ecosystem function. Ecology 88:1386–1394. https://doi.org/10.1890/06-0219.

Schinegger, R., Palt, M., Segurado, P., Schmutz, S., 2016. Untangling the effects of multiple human stressors and their impacts on fish assemblages in European running waters. Sci. Total Environ. 573:1079–1088. https://doi.org/10.1016/j.scitotenv.2016.08.143.

Segner, H., Sabater, S., 2014. Assessing the Impact of Multiple Stressors on Aquatic. The Receptor's Side Matters. Envirnmental Sci. Technol, Biota https://doi.org/10.1021/es405082t.

Smith, C.J., Osborn, A.M., 2009. Advantages and Limitations of Quantitative PCR (Q-PCR) -Based Approaches in Microbial Ecology. 67:pp. 6–20. https://doi.org/10.1111/j.1574-6941.2008.00629.x.

Tello, A., Austin, B., Telfer, T.C., 2012. Selective pressure of antibiotic pollution on bacteria of importance to public health. Environ. Health Perspect. 120, 1100–1106.

Timoner, X., Acuña, V., Von Schiller, D., Sabater, S., 2012. Functional responses of stream biofilms to flow cessation, desiccation and rewetting. Freshw. Biol. 57:1565–1578. https://doi.org/10.1111/j.1365-2427.2012.02818.x.

Tlili, A., Marechal, M., Montuelle, B., Volat, B., Dorigo, U., Bérard, A., 2011. Use of the MicroRespTM method to assess pollution-induced community tolerance to metals for lotic biofilms. Environ. Pollut. 159:18–24. https://doi.org/10.1016/j.envpol.2010.09.033.

Vinebrooke, R.D., Cottingham, K.L., Norberg, J., Scheffer, M., Dodson, S.I., Maberly, S.C., Sommer, U., 2004. Impacts of multiple stressors on biodiversity and ecosystem functioning: the role of species co-tolerance. Oikos 104:451–457. https://doi.org/10.1111/j.0030-1299.2004.13255.x.

Ylla, I., Sanpera-Calbet, I., Vázquez, E., Romaní, A.M., Muñoz, I., Butturini, A., Sabater, S., 2010. Organic matter availability during pre- and post-drought periods in a Mediterranean stream. Hydrobiologia 657:217–232. https://doi.org/10.1007/s10750-010-0193-z.

Ylla, I., Canhoto, C., Romaní, A.M., 2014. Effects of warming on stream biofilm organic matter use capabilities. Microb. Ecol. 68:132–145. https://doi.org/10.1007/s00248-014-0406-5.